Bias Estimation for Moving Optical Sensor Measurements with Targets of Opportunity

DJEDJIGA BELFADEL
RICHARD W. OSBORNE, III
YAAKOV BAR-SHALOM

Integration of space based sensors into a Ballistic Missile Defense System (BMDS) allows for detection and tracking of threats over a larger area than ground based sensors. This paper examines the effect of sensor bias error on the tracking quality of a Space Tracking and Surveillance System (STSS) for the highly non-linear problem of tracking a ballistic missile. The STSS constellation consists of two or more satellites (on known trajectories) for tracking ballistic targets. Each satellite is equipped with an IR sensor that provides azimuth and elevation to the target. The tracking problem is made more difficult due to a constant or slowly varying bias error present in each sensor's line of sight measurements. The measurements provided by these sensors are assumed time-coincident (synchronous) and perfectly associated. The Line Of Sight (LOS) measurements from the sensors are used to estimate simultaneously the Cartesian target of opportunity positions, and the sensor biases. The evaluation of the Cramér-Rao Lower Bound (CRLB) on the covariance of the bias estimates, which serves as a quantification of the available information about the biases, and the statistical tests on the results of simulations show that this method is statistically efficient, even for small sample sizes (as few as two sensors and six points on the (unknown) trajectory of a single target of opportunity). We also show that the Root Mean Square (RMS) position error is significantly improved with bias estimation compared with the target position estimation using the original biased measurements.

Manuscript received April 14, 2014; revised December 24, 2014; released for publication March 3, 2015.

Refereeing of this contribution was handled by Ramona Georgescu.

Approved for Public Release 14-MDA-7763 (27 March 14).

Partially funded by ARO W911NF-10-1-0369.

Authors' address: Electrical and Computer Engineering, University of Connecticut, Storrs, CT, U.S.A. (e-mail: djedjiga.belfadel@uconn.edu, rosborne@engr.uconn.edu, ybs@engr.uconn.edu).

I. INTRODUCTION

Space-based sensors can expand the range and effectiveness of the capabilities of a Ballistic Missile Defense System (BMDS) to counter future projected threats. A space based tracking system utilizing an IR sensor will allow detection and tracking of targets outside of terrestrial radar coverage. This is possible because a sensitive IR sensor in relatively close proximity can detect and track a target against the cold background of space. Multisensor systems use fusion of data from multiple sensors to form accurate estimates of a target track. To fuse multiple sensor data the individual sensor data must be expressed in a common reference frame. A problem encountered in multisensor systems is the presence of errors due to sensor bias. Some sources of bias errors include: measurement biases due to the deterioration of initial sensor calibration over time; attitude errors caused by biases in the gyros of the inertial measurement units of (airborne, seaborne, or spaceborne) sensors; and timing errors due to the biases in the onboard clock of each sensor platform [6].

In [6] time varying bias estimation based on a nonlinear least squares formulation and the singular value decomposition using truth data was presented. However, this work did not discuss the CRLB for bias estimation. An approach using maximum a posteriori (MAP) data association for concurrent bias estimation and data association based on sensor-level track state estimates was proposed in [7] and extended in [8].

Sensor calibration using in-situ celestial observations to estimate bias in space-based missile tracking was discussed in [5]. In [4] simultaneous sensor bias and targets position estimation using fixed passive sensors was presented. In the present paper, bias estimation is investigated when only targets of opportunity are available. The tracking system consists of two or three satellites tracking a ballistic target. We assume the sensors are synchronized, their locations are known, and the data association is correct; and we estimate their orientation biases. We investigate the use of the minimum possible number of moving sensors and measurements. Two cases are considered. In the first case, we use three moving optical sensors to estimate 3 points on the (unknown) trajectory of a single target of opportunity simultaneously with the biases of the three optical sensors [3]. In the second case, we estimate the position of 6 points on the trajectory of a single target of opportunity simultaneously with the biases of two space-based optical sensors[2]. First, we discuss the observability requirement related to the bias estimation. We evaluate the Cramér-Rao lower bound (CRLB) on the covariance of the bias estimates, which is the quantification of the available information on the sensor biases, and show via statistical tests that the estimation is statistically efficient—it meets the CRLB. Section II

presents the problem formulation and solution in detail. Section III describes the simulations performed and gives the results. Finally, Section IV gives the conclusions.

II. PROBLEM FORMULATION

The fundamental frame of reference used in this paper is the Earth Centered Inertial (ECI) Coordinate System. The ECI is defined by the orthogonal set of unit vectors $\{e_x, e_y, e_z\}$. The X-axis is directed toward the vernal Equinox, the Y-axis is in the equatorial plane and normal to the X-axis, and the Z-axis is directed along the rotation axis of the Earth (i.e., normal to the equatorial plane). In a multisensor scenario, sensor platform s will typically have a sensor reference frame associated with it (measurement frame of the sensor) defined by the orthogonal set of unit vectors $\{e_{\xi_s}, e_{\eta_s}, e_{\zeta_s}\}$. The origin of the measurement frame of the sensor is a translation of the ECI origin, and its axes are rotated with respect to the ECI axes. The rotation between these frames can be described by a set of Euler angles. We will refer to these angles $\phi_s + \phi_s^{\mathrm{n}}$, $\rho_s + \rho_s^{\mathrm{n}}$, $\psi_s + \psi_s^{\mathrm{n}}$ of sensor s as roll, pitch, and yaw respectively [6], where ϕ_s^{n} is the nominal roll angle, ϕ_s is the roll bias, etc.

Each angle defines a rotation about a prescribed axis, in order to align the sensor frame axes with the ECI axes. The xyz rotation sequence is chosen, which is accomplished by first rotating about the x axis by ϕ_s^{n}, then rotating about the y axis by ρ_s^{n}, and finally rotating about the z axis by ψ_s^{n}. The rotations sequence can be expressed by the matrices

$$
\begin{aligned}
T_s(\psi_s^{\mathrm{n}}, \rho_s^{\mathrm{n}}, \phi_s^{\mathrm{n}}) &= T_z(\psi_s^{\mathrm{n}}) \cdot T_y(\rho_s^{\mathrm{n}}) \cdot T_x(\phi_s^{\mathrm{n}}) \\
&= \begin{bmatrix} \cos\psi_s^{\mathrm{n}} & \sin\psi_s^{\mathrm{n}} & 0 \\ -\sin\psi_s^{\mathrm{n}} & \cos\psi_s^{\mathrm{n}} & 0 \\ 0 & 0 & 1 \end{bmatrix} \\
&\quad \cdot \begin{bmatrix} \cos\rho_s^{\mathrm{n}} & 0 & -\sin\rho_s^{\mathrm{n}} \\ 0 & 1 & 0 \\ \sin\rho_s^{\mathrm{n}} & 0 & \cos\rho_s^{\mathrm{n}} \end{bmatrix} \\
&\quad \cdot \begin{bmatrix} 1 & 0 & 0 \\ 0 & \cos\phi_s^{\mathrm{n}} & \sin\phi_s^{\mathrm{n}} \\ 0 & -\sin\phi_s^{\mathrm{n}} & \cos\phi_s^{\mathrm{n}} \end{bmatrix} \qquad (1)
\end{aligned}
$$

Assume there are N_S synchronized passive sensors, with known positions in ECI coordinates at times t_i, $\boldsymbol{\xi}_s(t_i) = [\xi_s(t_i), \eta_s(t_i), \zeta_s(t_i)]'$, $s = 1, 2, \ldots, N_S$, and N_t target locations at $\mathbf{x}(t_i) = [x(t_i), y(t_i), z(t_i)]'$, $i = 1, 2, \ldots, N_t$, also in ECI coordinates. We assume that each sensor sees all the target locations (same physical target at different times).[1] With the previous convention, the operations

[1]This can also be different targets at a common time or at different times, as long as the sensors are synchronized.

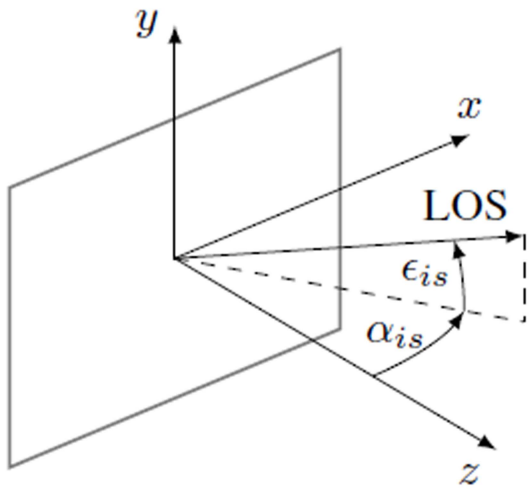

Fig. 1. Optical sensor coordinate system with the origin in the center of the focal plane.

needed to transform the position of a given target location at t_i expressed in ECI coordinates into the sensor s coordinate system (based on its nominal orientation) is

$$
\begin{aligned}
\mathbf{x}_s^{\mathrm{n}}(t_i) &= T(\boldsymbol{\omega}_s(t_i))(\mathbf{x}(t_i) - \boldsymbol{\xi}_s(t_i)) \\
&\quad i = 1, 2, \ldots, N_t, \ s = 1, 2, \ldots, N_S \qquad (2)
\end{aligned}
$$

where $\boldsymbol{\omega}_s(t_i) = [\phi_s^{\mathrm{n}}(t_i), \rho_s^{\mathrm{n}}(t_i), \psi_s^{\mathrm{n}}(t_i)]'$ is the nominal orientation of sensor s at times t_i, $T(\boldsymbol{\omega}_s(t_i))$ is the appropriate rotation matrix, and the translation $(\mathbf{x}(t_i) - \boldsymbol{\xi}_s(t_i))$ is the difference between the vector position of the target i and the vector position of the sensor s, both expressed in ECI coordinates. The superscript "n" in (2) indicates that the rotation matrix is based on the nominal sensor orientation.

As shown in Figure 1, the azimuth angle $\alpha_s(t_i)$ is the angle in the sensor xz plane between the sensor z axis and the line of sight to the target, while the elevation angle $\epsilon_s(t_i)$ is the angle between the line of sight to the target and its projection onto the xz plane, i.e.,

$$
\begin{bmatrix} \alpha_s(t_i) \\ \epsilon_s(t_i) \end{bmatrix} = \begin{bmatrix} \tan^{-1}\left(\dfrac{x_s(t_i)}{z_s(t_i)}\right) \\ \tan^{-1}\left(\dfrac{y_s(t_i)}{\sqrt{x_s^2(t_i) + z_s^2(t_i)}}\right) \end{bmatrix} \qquad (3)
$$

The model for the biased noise-free LOS measurements is then

$$
\begin{aligned}
\begin{bmatrix} \boldsymbol{\alpha}_s^b(t_i) \\ \boldsymbol{\epsilon}_s^b(t_i) \end{bmatrix} &= \begin{bmatrix} g_1(\mathbf{x}(t_i), \boldsymbol{\xi}_s(t_i), \boldsymbol{\omega}_s(t_i), \mathbf{b}_s) \\ g_2(\mathbf{x}(t_i), \boldsymbol{\xi}_s(t_i), \boldsymbol{\omega}_s(t_i), \mathbf{b}_s) \end{bmatrix} \\
&\triangleq \mathbf{g}(\mathbf{x}(t_i), \boldsymbol{\xi}_s(t_i), \boldsymbol{\omega}_s(t_i), \mathbf{b}_s) \qquad (4)
\end{aligned}
$$

where g_1 and g_2 denote the sensor Cartesian coordinates-to-azimuth/elevation angle mapping that can be found by inserting (2) and (3) into (4), and the bias vector of

sensor s is

$$\mathbf{b}_s = [\phi_s, \rho_s, \psi_s]' \tag{5}$$

For a given target, each sensor provides the noisy LOS measurements

$$\mathbf{z}_s(t_i) = \mathbf{g}(\mathbf{x}(t_i), \boldsymbol{\xi}_s(t_i), \boldsymbol{\omega}_s(t_i), \mathbf{b}_s) + \mathbf{w}_s(t_i) \tag{6}$$

where

$$\mathbf{w}_s(t_i) = [w_s^{\alpha}(t_i), w_s^{\epsilon}(t_i)]' \tag{7}$$

The measurement noises $\mathbf{w}_s(t_i)$ are zero-mean, white Gaussian with

$$R_s = \begin{bmatrix} (\sigma_s^{\alpha})^2 & 0 \\ 0 & (\sigma_s^{\epsilon})^2 \end{bmatrix} \tag{8}$$

and are assumed mutually independent. The problem is to estimate the bias vectors for all sensors and the locations of the targets of opportunity. We shall obtain the maximum likelihood (ML) estimate of the augmented parameter vector

$$\boldsymbol{\theta} = [\mathbf{x}(t_1)', \ldots, \mathbf{x}(t_{N_t})', \mathbf{b}_1', \ldots, \mathbf{b}_{N_S}']' \tag{9}$$

consisting of the (unknown) target locations and sensor biases, by maximizing the likelihood function (LF) of $\boldsymbol{\theta}$

$$\Lambda(\boldsymbol{\theta}) = \prod_{i=1}^{N_t} \prod_{s=1}^{N_S} p(\mathbf{z}_s(t_i) \mid \boldsymbol{\theta}) \tag{10}$$

where

$$p(\mathbf{z}_s(t_i) \mid \boldsymbol{\theta}) = |2\pi R_s|^{-1/2} \cdot \exp(-\tfrac{1}{2}[\mathbf{z}_s(t_i) - \mathbf{h}_{is}(\boldsymbol{\theta})]' R_s^{-1} [\mathbf{z}_s(t_i) - \mathbf{h}_{is}(\boldsymbol{\theta})]) \tag{11}$$

and we use the compact notation

$$\mathbf{h}_{is}(\boldsymbol{\theta}) \stackrel{\Delta}{=} \mathbf{g}(\mathbf{x}(t_i), \boldsymbol{\xi}_s(t_i), \boldsymbol{\omega}_s(t_i), \mathbf{b}_s) \tag{12}$$

The ML estimate (MLE) is then

$$\hat{\boldsymbol{\theta}}^{ML} = \arg\max_{\boldsymbol{\theta}} \Lambda(\boldsymbol{\theta}) \tag{13}$$

In order to find the MLE, one has to solve a nonlinear least squares problem for the exponent in (11). This will be done using a numerical search via the Iterated Least Squares (ILS) technique [1].

A. Requirements for Bias Estimability

Minimum number of measurements. The number of equations (size of the measurement vector) has to be at least equal to the number of parameters to be estimated (target location and bias components). Each passive sensor provides two-dimensional measurement (the two LOS angles to the target), and it is assumed that each sensor sees all the target locations at a common time. Stacking together each measurement of N_t target locations seen by N_S sensors results in an overall measurement vector of dimension $2N_tN_S$. Therefore we must have

$$2N_tN_S \geq 3(N_t + N_S) \tag{14}$$

This is a necessary condition but not sufficient because (13) has to have a unique solution, i.e., the parameter vector has to be estimable [1].

Invertibility of the Fisher Information matrix (FIM). In order to have parameter observability, the FIM must be invertible. If the FIM is not invertible (i.e., it is singular), then the CRLB (the inverse of the FIM) will not exist—the FIM will have one or more infinite eigenvalues, which means total uncertainty in a subspace of the parameter space, i.e., ambiguity [2].

For the examples of bias estimability discussed in the sequel, to estimate the biases of 3 sensors (9 bias components) we need 3 target locations (9 position components), i.e., the search is in an 18-dimensional space, while for 2 sensors (6 bias components) we need at least 6 target locations (18 position components) in order to meet the necessary requirement (14). As stated previously, the FIM must be invertible, so the rank of the FIM has to be equal to the number of parameters to be estimated (9 + 9 = 18, or 6 + 18 = 24, in the previous examples). The full rank of the FIM is a necessary and sufficient condition for estimability.

B. Iterated Least Squares for Maximization of the LF of $\boldsymbol{\theta}$

Given the estimate $\hat{\boldsymbol{\theta}}^j$ after j iterations, the ILS estimate after the $(j+1)$th iteration will be

$$\hat{\boldsymbol{\theta}}^{j+1} = \hat{\boldsymbol{\theta}}^j + [(H^j)' R^{-1} H^j]^{-1} (H^j)' R^{-1} [\mathbf{z} - \mathbf{h}(\hat{\boldsymbol{\theta}}^j)] \tag{15}$$

where

$$\mathbf{z} = [z_1(t_1)', \ldots, z_s(t_1)', \ldots, z_s(t_i)', \ldots, z_{N_S}(t_{N_t})']' \tag{16}$$

$$\mathbf{h}(\hat{\boldsymbol{\theta}}^j) = [h_{11}(\hat{\boldsymbol{\theta}}^j)', \ldots, h_{is}(\hat{\boldsymbol{\theta}}^j)', \ldots, h_{N_tN_S}(\hat{\boldsymbol{\theta}}^j)'] \tag{17}$$

$$R = \begin{bmatrix} R_1 & 0 & \cdots & 0 \\ 0 & R_2 & \cdots & 0 \\ \vdots & \vdots & \ddots & \vdots \\ 0 & \cdots & 0 & R_{N_S} \end{bmatrix} \tag{18}$$

where R_s is the measurement noise covariance matrix of sensor s, and

$$H^j = \left. \frac{\partial \mathbf{h}(\boldsymbol{\theta}^j)}{\partial \boldsymbol{\theta}} \right|_{\boldsymbol{\theta} = \hat{\boldsymbol{\theta}}^j} \tag{19}$$

is the Jacobian matrix of the vector consisting of the stacked measurement functions (17) w.r.t. (9) evaluated at the ILS estimate from the previous iteration j. In this case, the Jacobian matrix is, with the iteration index omitted for conciseness,

$$H = [H_{11} \quad H_{21} \cdots H_{N_t1} \quad H_{12} \cdots H_{N_tN_S}]' \tag{20}$$

where

$$H_{is} = \begin{bmatrix} \frac{\partial g_{1s}(t_i)}{\partial x(t_1)} & \frac{\partial g_{2s}(t_i)}{\partial x(t_1)} \\ \frac{\partial g_{1s}(t_i)}{\partial y(t_1)} & \frac{\partial g_{2s}(t_i)}{\partial y(t_1)} \\ \frac{\partial g_{1s}(t_i)}{\partial z(t_1)} & \frac{\partial g_{2s}(t_i)}{\partial z(t_1)} \\ \vdots & \vdots \\ \frac{\partial g_{1s}(t_i)}{\partial x(t_{N_t})} & \frac{\partial g_{2s}(t_i)}{\partial x(t_{N_t})} \\ \frac{\partial g_{1s}(t_i)}{\partial y(t_{N_t})} & \frac{\partial g_{2s}(t_i)}{\partial y(t_{N_t})} \\ \frac{\partial g_{1s}(t_i)}{\partial z(t_{N_t})} & \frac{\partial g_{2s}(t_i)}{\partial z(t_{N_t})} \\ \frac{\partial g_{1s}(t_i)}{\partial \psi_1} & \frac{\partial g_{2s}(t_i)}{\partial \psi_1} \\ \frac{\partial g_{1s}(t_i)}{\partial \rho_1} & \frac{\partial g_{2s}(t_i)}{\partial \rho_1} \\ \frac{\partial g_{1s}(t_i)}{\partial \phi_1} & \frac{\partial g_{2s}(t_i)}{\partial \phi_1} \\ \vdots & \vdots \\ \frac{\partial g_{1s}(t_i)}{\partial \psi_{N_S}} & \frac{\partial g_{2s}(t_i)}{\partial \psi_{N_S}} \\ \frac{\partial g_{1s}(t_i)}{\partial \rho_{N_S}} & \frac{\partial g_{2s}(t_i)}{\partial \rho_{N_S}} \\ \frac{\partial g_{1s}(t_i)}{\partial \phi_{N_S}} & \frac{\partial g_{2s}(t_i)}{\partial \phi_{N_S}} \end{bmatrix} \tag{21}$$

The appropriate partial derivatives are given in the appendix.

C. Initialialization

In order to perform the numerical search via ILS, an initial estimate $\hat{\boldsymbol{\theta}}^0$ is required. Assuming that the biases are null, the LOS measurements from the first and the second sensor $\alpha_1(t_i)$, $\alpha_2(t_i)$, and $\epsilon_1(t_i)$ can be used to solve for each initial Cartesian target position, in ECI coordinates, using (22)–(24).

$$x(t_i)^0 = \frac{\xi_2(t_i) - \xi_1(t_i) + \zeta_1(t_i)\tan\alpha_1(t_i) - \zeta_2(t_i)\tan\alpha_2(t_i)}{\tan\alpha_1(t_i) - \tan\alpha_2(t_i)} \tag{22}$$

$$y(t_i)^0 = \frac{\tan\alpha_1(t_i)(\xi_2(t_i) + \tan\alpha_2(t_i)(\zeta_1(t_i) - \zeta_2(t_i))) - \xi_1(t_i)\tan\alpha_2(t_i)}{\tan\alpha_1(t_i) - \tan\alpha_2(t_i)} \tag{23}$$

$$z(t_i)^0 = \eta_1(t_i) + \tan\epsilon_1(t_i)\left|\frac{(\xi_1(t_i) - \xi_2(t_i))\cos\alpha_2(t_i) + (\zeta_2(t_i) - \zeta_1(t_i))\sin\alpha_2(t_i)}{\sin(\alpha_1(t_i) - \alpha_2(t_i))}\right| \tag{24}$$

D. Cramér-Rao Lower Bound

In order to evaluate the efficiency of the estimator, the CRLB must be calculated. The CRLB provides a lower bound on the covariance matrix of an unbiased estimator as [1]

$$E\{(\boldsymbol{\theta} - \hat{\boldsymbol{\theta}})(\boldsymbol{\theta} - \hat{\boldsymbol{\theta}})'\} \geq J(\boldsymbol{\theta})^{-1} \tag{25}$$

where J is the Fisher Information Matrix (FIM), $\boldsymbol{\theta}$ is the true parameter vector to be estimated, and $\hat{\boldsymbol{\theta}}$ is the estimate. The FIM is

$$J(\boldsymbol{\theta}) = E\{[\nabla_{\boldsymbol{\theta}} \ln\Lambda(\boldsymbol{\theta})][\nabla_{\boldsymbol{\theta}} \ln\Lambda(\boldsymbol{\theta})]'\}|_{\boldsymbol{\theta}=\boldsymbol{\theta}_{\text{true}}} \tag{26}$$

where the gradient of the log-likelihood function is

$$\lambda(\boldsymbol{\theta}) \triangleq \ln\Lambda(\boldsymbol{\theta}) \tag{27}$$

$$\nabla_{\boldsymbol{\theta}}\lambda(\boldsymbol{\theta}) = \sum_{i=1}^{N_t}\sum_{s=1}^{N_S} H_{is}' R_s^{-1}(\mathbf{z}_s(t_i) - \mathbf{h}_{is}(\boldsymbol{\theta})) \tag{28}$$

which, when plugged into (26), gives

$$\begin{aligned} J(\boldsymbol{\theta}) &= \sum_{i=1}^{N_t}\sum_{s=1}^{N_S} H_{is}'(R_s^{-1})H_{is}|_{\boldsymbol{\theta}=\boldsymbol{\theta}_{\text{true}}} \\ &= H'(R^{-1})H|_{\boldsymbol{\theta}=\boldsymbol{\theta}_{\text{true}}} \end{aligned} \tag{29}$$

Since $\boldsymbol{\theta}_{\text{true}}$ is not available in practice, J will be evaluated at the estimate, and, as it's pointed out later, the two results are practically the same.

E. Test for Efficiency with Monte Carlo Runs

The Normalized Estimation Error Squared (NEES) for the parameter θ (under the hypothesis of efficiency), defined as

$$\epsilon_\theta = (\theta - \hat{\theta})'P^{-1}(\theta - \hat{\theta}) = (\theta - \hat{\theta})'J(\theta)(\theta - \hat{\theta}) \tag{30}$$

is chi-square distributed with n_x (the dimension of θ) degrees of freedom, that is,

$$\epsilon_\theta \sim \chi^2_{n_x} \tag{31}$$

The hypothesis test for efficiency whether (31) can be accepted, i.e., that $P = J^{-1}$ is discussed in [2] and outlined next. The NEES is used in simulations to check whether the estimator is efficient, that is, the errors are statistically consistent with the covariance given by the CRLB—this is the efficiency check. Thus the efficiency

check of the estimator (in simulation—because this is the only situation where θ is available) consists of verifying whether (31) holds. The practical procedure to check the estimator efficiency is using the sample average NEES from N independent Monte Carlo runs defined as

$$\bar{\epsilon}_x = \frac{1}{N}\sum_{i=1}^{N}\epsilon_x^i \tag{32}$$

The quantity $N\bar{\epsilon}$ is chi-square distributed with Nn_x degrees of freedom.

Let the $1-Q$ (Q is the type I error probability of the test) two-sided probability region for $N\bar{\epsilon}$ be the interval $[\epsilon_1', \epsilon_2']$.

$$\epsilon_1' = \chi^2_{Nn_x}\left(\frac{Q}{2}\right) \tag{33}$$

$$\epsilon_2' = \chi^2_{Nn_x}\left(1-\frac{Q}{2}\right) \tag{34}$$

where in view of the division by N in (32), one has

$$\epsilon_i = \frac{\epsilon_i'}{N} \tag{35}$$

Thus, if the estimator is efficient, one has to have

$$P\{\bar{\epsilon}_x \in [\epsilon_1', \epsilon_2']\} = 1-Q \tag{36}$$

III. SIMULATIONS

We simulate a space based tracking system tracking a ballistic missile. The missile and satellite trajectories are generated using System Tool Kit (STK).[2] The target modeled represents a ballistic missile with a flight time of about 20 minutes. STK provides the target and sensor positions in three dimensional Cartesian coordinates at 1 s intervals. The target launch time is chosen so that the satellite sensors were able to follow the missile trajectory throughout its flight path.

A. Three-Sensor Case

We simulated three space based optical sensors at various known orbits observing a target at three points in time at unknown locations. In this case, an 18-dimensional parameter vector is to be estimated. Figure 2 shows each target position observed by the sensors (Figure 3 gives an image of this). As discussed in the previous section, the three sensor biases are roll, pitch, and yaw angle offsets. The biases for each sensor were set to 0.5° = 8.72 mrad. We ran 100 Monte Carlo runs. In order to establish a baseline for evaluating the performance of our algorithm, we also ran the simulations without biases, and with biases but without bias estimation. The horizontal and vertical fields-of-view of each sensor are assumed to be 60°. The measurement noise standard deviation σ_s (identical across sensors for both azimuth and elevation measurements, $\sigma_s^\alpha = \sigma_s^\epsilon = \sigma_s$) was assumed to be 30 μrad.

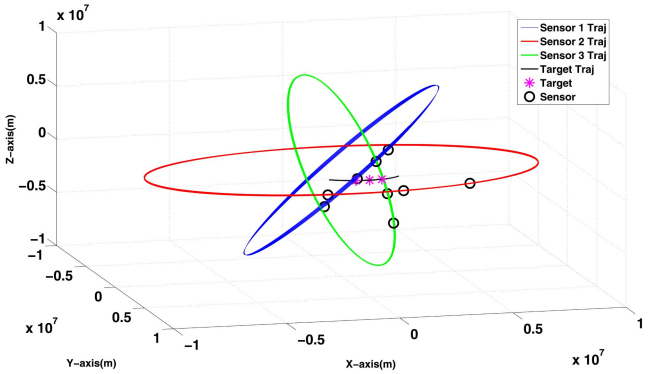

Fig. 2. Target and satellite trajectories for the three-sensor case.

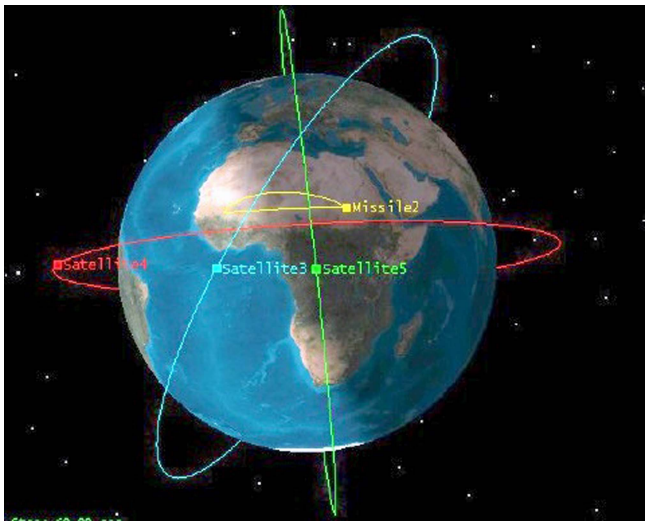

Fig. 3. Target and satellite trajectories for the three-sensor case.

1) Description of the scenarios. The sensors are assumed to provide LOS angle measurements. We denote by $\boldsymbol{\xi}_1, \boldsymbol{\xi}_2, \boldsymbol{\xi}_3$ the 3D Cartesian sensor locations, and $\mathbf{x}(t_1), \mathbf{x}(t_2), \mathbf{x}(t_3)$ the 3D Cartesian target locations (all in ECI). The three target locations were chosen from a trajectory of a ballistic target as follows (in km)

$$\mathbf{x}(t_1) = [7{,}518 \quad -1{,}311 \quad -1{,}673]' \tag{37}$$

$$\mathbf{x}(t_2) = [7{,}942 \quad -509 \quad -1{,}375]' \tag{38}$$

$$\mathbf{x}(t_3) = [7{,}988 \quad 317 \quad -1{,}012]' \tag{39}$$

Table I summarizes the sensor positions (in km).

2) Statistical efficiency of the estimates. In order to test for the statistical efficiency of the estimate (of the 18 dimensional vector (9)), the NEES [1] is used, with the CRLB as the covariance matrix. The sample average NEES over 100 Monte Carlo runs calculated using the FIM evaluated at the true bias values and target locations is approximately 17.3, and the sample average NEES calculated using the FIM evaluated at the estimated biases and target locations is approximately 17.6 and both fall in the interval given below. According to

[2]STK Systems Tool Kit are registered trademarks of Analytical Graphics, Inc.

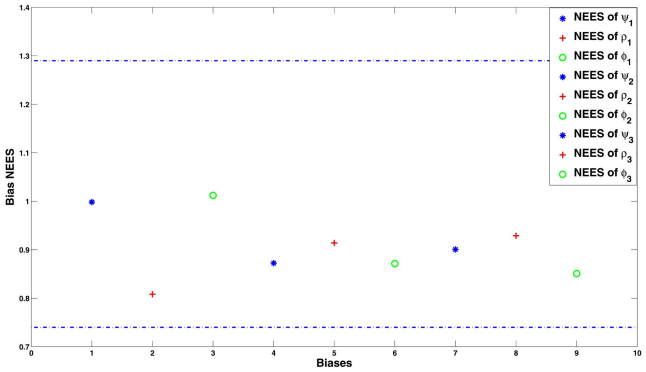

Fig. 4. Sample average bias NEES (CRLB evaluated at the estimate), for each of the 9 biases, over 100 Monte Carlo runs (Three-sensor case).

TABLE I
Sensor positions (km).

	t_1	t_2	t_3
ξ_1	1,235	1,062	887
η_1	158	−174	−507
ζ_1	6,927	6,955	6,963
ξ_2	5,549	3,061	112
η_2	1,116	2,993	4,418
ζ_2	6,285	7,295	7,212
ξ_3	6,499	7,897	8,389
η_3	−279	−719	−1,074
ζ_3	−5,407	−2,944	−143

the CRLB, the FIM has to be evaluated at the true parameter. Since this is not available in practice, however, it is useful to evaluate the FIM also at the estimated parameter, the only one available in real world implementations [9], [10]. The results are very close regardless of which values are chosen for evaluation of the FIM. The 95% probability region for the 100 sample average NEES of the 18 dimensional parameter vector is $[16.84, 19.19]'$. This NEES is found to be within this interval and the MLE is therefore statistically efficient. Figure 4 shows the individual bias component NEES, The 95% probability region for the 100 sample average single component NEES is $[0.74, 1.29]'$. The NEES values are found to be within this interval.

The RMS position errors for the 3 target locations are summarized in Table II. In this table, the first estimation scheme was established as a baseline using bias-free LOS measurements to estimate the target locations.[3] For the second scheme, we used biased LOS measurements but we only estimated target locations. In the last scheme, we used biased LOS measurements and we simultaneously estimated the target locations and sensor biases. Bias estimation yields significantly

[3]As shown in [9], [10] the unbiased LOS measurements yield composite measurements (full position MLEs) whose errors are zero-mean and their covariance is equal to the corresponding CRLB.

TABLE II
Sample average position RMSE (m) for the 3 targets, over 100 Monte Carlo runs, for the 3 estimation schemes (Three-sensor case).

Scheme	1	2	3
First Target	127	69,391	673
Second Target	98	41,713	484
Third Target	82	16,271	343

TABLE III
Sample average bias (μrad) RMSE over 100 Monte Carlo runs and the corresponding bias standard deviation from the CRLB (Three-sensor case).

	RMSE	σ_{CRLB}
ψ_1	138.009	138.211
ρ_1	176.073	195.808
ϕ_1	150.108	149.209
ψ_2	178.507	191.110
ρ_2	147.752	154.675
ϕ_2	230.009	246.231
ψ_3	229.131	241.389
ρ_3	134.680	139.726
ϕ_3	708.588	768.215

TABLE IV
Sample average bias (μrad) error $\bar{\tilde{b}}$ over 100 Monte Carlo runs (Three-sensor case).

	$\bar{\tilde{b}}$	$2\frac{\sigma_{\text{CRLB}}}{\sqrt{N}}$
ψ_1	−1.728	27.642
ρ_1	16.945	39.161
ϕ_1	4.545	29.841
ψ_2	−17.323	38.222
ρ_2	5.262	30.935
ϕ_2	22.804	49.246
ψ_3	20.580	48.277
ρ_3	−7.454	27.945
ϕ_3	79.386	153.643

improved target RMS position errors in the presence of biases.

Each component of $\boldsymbol{\theta}$ should also be individually consistent with its corresponding σ_{CRLB} (the square root of the corresponding diagonal element of the inverse of the FIM). In this case, the sample average bias RMSE over 100 Monte Carlo runs should be within 15% of its corresponding bias standard deviation from the CRLB (σ_{CRLB}) with 95% probability. Table III demonstrates the consistency of the individual bias estimates. This complements the NEES evaluations from Figure 4.

To confirm that the bias estimates are unbiased, the average bias error $\bar{\tilde{b}}$, from Table IV (over 100 Monte Carlo runs) confirms that $|\bar{\tilde{b}}|$ is less then $2\sigma_{\text{CRLB}}/\sqrt{N}$ (which it should hold with 95% probability), i.e., these estimates are unbiased.

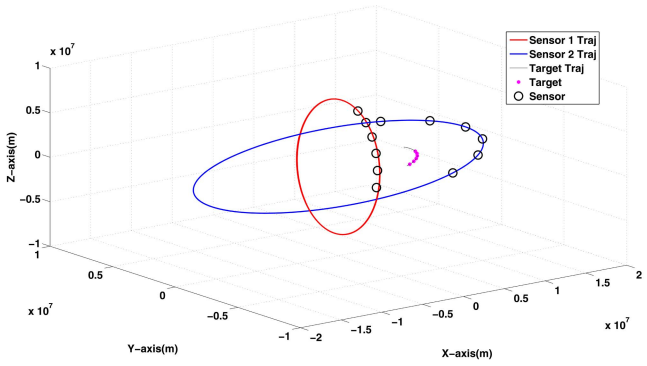

Fig. 5. Target and satellite trajectories for the two-sensor case

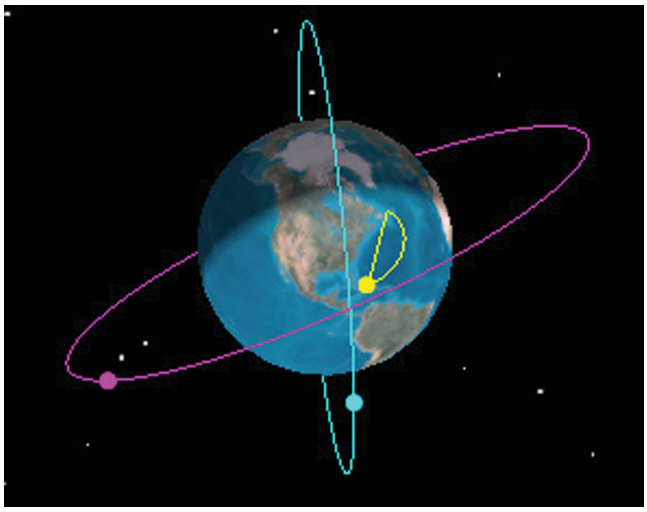

Fig. 6. Target and satellite trajectories for the two-sensor case

B. Two-Sensor Case

We simulated two space-based optical sensors at various known orbits observing a target at six (unknown) locations (which is equivalent to viewing six different targets at unknown locations). In this case, a 24-dimensional parameter vector is to be estimated. As shown in Figure 5, each target position can be observed by all sensors. As discussed in the previous section, the three sensor biases were roll, pitch and yaw angle offsets. All the biases for each sensor were set to 50 μrad.

We made 100 Monte Carlo runs. In order to establish a baseline for evaluating the performance of our algorithm, we also ran the simulations without bias, and with bias but without bias estimation. The measurement noise standard deviation σ_s (identical across sensors for both azimuth and elevation measurements) was assumed to be 30 μrad.

1) Description of the scenarios. The sensors are assumed to provide LOS angle measurements. We denote by $\boldsymbol{\xi}_1, \boldsymbol{\xi}_2$ the 3D Cartesian sensor positions at six different times, and $\mathbf{x}(t_1), \mathbf{x}(t_2)$, $\mathbf{x}(t_3), \mathbf{x}(t_4)$, $\mathbf{x}(t_5), \mathbf{x}(t_6)$ the six 3D Cartesian target locations (all in ECI). The six target locations were chosen from a trajectory of a ballistic target as follows (in km)

TABLE V
Sensor positions (km).

	t_1	t_2	t_3	t_4	t_5	t_6
ξ_1	187	−902	−1,934	−2,840	−3,559	−4,046
η_1	−1,439	−2,786	−3,951	−4,858	−5,447	−5,680
ζ_1	6,886	6,400	5,494	4,229	2,687	968
ξ_2	−3,966	123	4,195	7,646	9,965	10,810
η_2	−5,969	−7,238	−7,436	−6,533	−4,664	−2,105
ζ_2	8,519	8,458	7,145	4,774	1,698	−1,630

$$\mathbf{x}(t_1) = [-1{,}167 \quad -5{,}782 \quad 3{,}028]' \tag{40}$$

$$\mathbf{x}(t_2) = [-1{,}054 \quad -6{,}027 \quad 3{,}436]' \tag{41}$$

$$\mathbf{x}(t_3) = [-922 \quad -6{,}148 \quad 3{,}772]' \tag{42}$$

$$\mathbf{x}(t_4) = [-774 \quad -6{,}155 \quad 4{,}036]' \tag{43}$$

$$\mathbf{x}(t_5) = [-611 \quad -6{,}056 \quad 4{,}228]' \tag{44}$$

$$\mathbf{x}(t_6) = [-435 \quad -5{,}852 \quad 4{,}344]' \tag{45}$$

Table V summarizes the sensor positions.

2) Statistical Efficiency of the Estimates. In order to test for the statistical efficiency of the estimate (of the 24 dimensional vector), the NEES is used, with the CRLB as the covariance matrix. The sample average NEES over 100 Monte Carlo runs calculated using the FIM evaluated at the true bias values and target locations is approximately 23.995, and the sample average NEES calculated using the FIM evaluated at the estimated biases and target locations is approximately 23.996 and both fall in the interval given below. The results are practically identical regardless of which values are chosen for evaluation of the FIM. The 95% probability region for the 100 sample average NEES of the 24 dimensional parameter vector is $[22.66, 25.37]'$. This NEES is found to be within this interval and the MLE is therefore statistically efficient. Figure 7 shows the individual bias component NEES. The 95% probability region for the 100 sample average single component NEES is $[0.74, 1.29]'$. These NEES are found to be within this interval, except for one component, which is slightly outside this region.

The RMS position errors for the 6 target locations are summarized in Table VI. In this table, the first estimation scheme was established as a baseline using bias-free LOS measurements to estimate the target locations. For the second scheme, we used biased LOS measurements but we only estimated target locations. In the last scheme, we used biased LOS measurements and we simultaneously estimated the target locations and sensor biases. Once again, bias estimation yields significantly improved target RMS position errors in the presence of biases.

Each component of $\boldsymbol{\theta}$ should also be individually consistent with its corresponding σ_{CRLB} (the square root of the corresponding diagonal element of the inverse

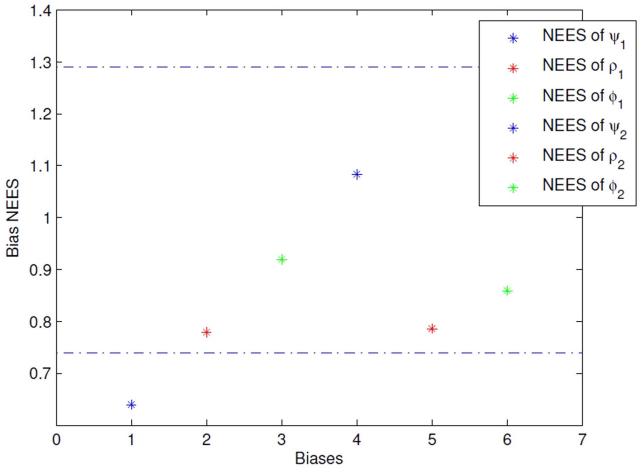

Fig. 7. Sample average bias NEES (CRLB evaluated at the estimate), for each of the 6 biases, over 100 Monte Carlo runs (Two-sensor case).

TABLE VI
Sample average position RMSE (m) for the 6 targets, over 100 Monte Carlo runs, for the 3 estimation schemes (Two-sensor case).

Scheme	1	2	3
First Target	234	93,123	521
Second Target	235	70,902	417
Third Target	212	60,840	403
Fourth Target	501	57,113	677
Fifth Target	637	262,712	754
Sixth Target	580	163,104	703

of FIM). In this case, the sample average bias RMSE over 100 Monte Carlo runs should be within 15% of its corresponding bias standard deviation from the CRLB (σ_{CRLB}) with 95% probability. Table VII demonstrates the efficiency of the individual bias estimates.

To confirm that the bias estimates are unbiased, the average bias error $\bar{\tilde{b}}$, from Table VIII, over 100 Monte Carlo runs confirms that $|\bar{\tilde{b}}|$ is less then $2\sigma_{\text{CRLB}}/\sqrt{N}$ (which it should hold with 95% probability), i.e., these estimates are unbiased.

IV. CONCLUSIONS AND FUTURE WORK

Previous research into the simultaneous estimation of the 3D Cartesian locations of the targets of opportunity and the angle measurement biases of fixed sensors [4] demonstrated that the maximum likelihood estimator via the ILS algorithm was able to provide statistically efficient estimates. In the three-sensor case it was shown that one has complete observability of the sensor biases. In the two-sensor case a rank deficiency of 1 in the FIM was observed. A suitable geometric explanation was provided for this. In the present paper we presented a new algorithm that uses targets of opportunity for estimation of measurement biases for moving sensors. The first step was formulating a general bias model for synchronized space-based (moving) optical sensors

TABLE VII
Sample average bias (μrad) RMSE over 100 Monte Carlo runs and the corresponding bias standard deviation from the CRLB (Two-sensor case).

	RMSE	σ_{CRLB}
ψ_1	74.945	72.334
ρ_1	108.100	99.322
ϕ_1	88.624	81.117
ψ_2	53.548	52.208
ρ_2	25.491	30.455
ϕ_2	140.719	98.743

TABLE VIII
Sample average bias (mrad) error $\bar{\tilde{b}}$ over 100 Monte Carlo runs (Two-sensor case).

	$\bar{\tilde{b}}$	$\frac{\sigma_{\text{CRLB}}}{\sqrt{N}}$
ψ_1	−27.248	19.750
ρ_1	−13.943	21.213
ϕ_1	0.289	17.705
ψ_2	−9.677	12.289
ρ_2	5.167	0.654
ϕ_2	10.985	19.217

at known locations. The association of measurements is assumed to be perfect. Based on this, we used a ML approach that led to a nonlinear least-squares estimation problem for simultaneous estimation of the 3D Cartesian locations of the targets of opportunity and the angle measurement biases of the sensors. The bias estimates, obtained via ILS, were shown to be unbiased and statistically efficient for all the scenarios considered.

APPENDIX

The appropriate partial derivatives of (21) are

$$\frac{\partial g_{1s}(t_i)}{\partial x(t_k)} = \frac{\partial g_{1s}(t_i)}{\partial x_s(t_i)}\frac{\partial x_s(t_i)}{\partial x(t_k)} + \frac{\partial g_{1s}(t_i)}{\partial y_s(t_i)}\frac{\partial y_s(t_i)}{\partial x(t_k)} + \frac{\partial g_{1s}(t_i)}{\partial z_s(t_i)}\frac{\partial z_s(t_i)}{\partial x(t_k)} \tag{46}$$

$$\frac{\partial g_{1s}(t_i)}{\partial y(t_k)} = \frac{\partial g_{1s}(t_i)}{\partial x_s(t_i)}\frac{\partial x_s(t_i)}{\partial y(t_k)} + \frac{\partial g_{1s}(t_i)}{\partial y_s(t_i)}\frac{\partial y_s(t_i)}{\partial y(t_k)} + \frac{\partial g_{1s}(t_i)}{\partial z_s(t_i)}\frac{\partial z_s(t_i)}{\partial y(t_k)} \tag{47}$$

$$\frac{\partial g_{1s}(t_i)}{\partial z(t_k)} = \frac{\partial g_{1s}(t_i)}{\partial x_s(t_i)}\frac{\partial x_s(t_i)}{\partial z(t_k)} + \frac{\partial g_{1s}(t_i)}{\partial y_s(t_i)}\frac{\partial y_s(t_i)}{\partial z(t_k)} + \frac{\partial g_{1s}(t_i)}{\partial z_s(t_i)}\frac{\partial z_s(t_i)}{\partial z(t_k)} \tag{48}$$

$$\frac{\partial g_{1s}(t_i)}{\partial \psi_k} = \frac{\partial g_{1s}(t_i)}{\partial x_s(t_i)}\frac{\partial x_s(t_i)}{\partial \psi_k} + \frac{\partial g_{1s}(t_i)}{\partial y_s(t_i)}\frac{\partial y_s(t_i)}{\partial \psi_k} + \frac{\partial g_{1s}(t_i)}{\partial z_s(t_i)}\frac{\partial z_s(t_i)}{\partial \psi_k} \tag{49}$$

$$\frac{\partial g_{1s}(t_i)}{\partial \rho_k} = \frac{\partial g_{1s}(t_i)}{\partial x_s(t_i)}\frac{\partial x_s(t_i)}{\partial \rho_k} + \frac{\partial g_{1s}(t_i)}{\partial y_s(t_i)}\frac{\partial y_s(t_i)}{\partial \rho_k} + \frac{\partial g_{1s}(t_i)}{\partial z_s(t_i)}\frac{\partial z_s(t_i)}{\partial \rho_k} \tag{50}$$

$$\frac{\partial g_{1s}(t_i)}{\partial \phi_k} = \frac{\partial g_{1s}(t_i)}{\partial x_s(t_i)}\frac{\partial x_s(t_i)}{\partial \phi_k} + \frac{\partial g_{1s}(t_i)}{\partial y_s(t_i)}\frac{\partial y_s(t_i)}{\partial \phi_k} + \frac{\partial g_{1s}(t_i)}{\partial z_s(t_i)}\frac{\partial z_s(t_i)}{\partial \phi_k} \tag{51}$$

$$\frac{\partial g_{2s}(t_i)}{\partial x(t_k)} = \frac{\partial g_{2s}(t_i)}{\partial x_s(t_i)}\frac{\partial x_s(t_i)}{\partial x(t_k)} + \frac{\partial g_{2s}(t_i)}{\partial y_s(t_i)}\frac{\partial y_s(t_i)}{\partial x(t_k)} + \frac{\partial g_{2s}(t_i)}{\partial z_s(t_i)}\frac{\partial z_s(t_i)}{\partial x(t_k)} \tag{52}$$

$$\frac{\partial g_{2s}(t_i)}{\partial y(t_k)} = \frac{\partial g_{2s}(t_i)}{\partial x_s(t_i)}\frac{\partial x_s(t_i)}{\partial y(t_k)} + \frac{\partial g_{2s}(t_i)}{\partial y_s(t_i)}\frac{\partial y_s(t_i)}{\partial y(t_k)} + \frac{\partial g_{2s}(t_i)}{\partial z_s(t_i)}\frac{\partial z_s(t_i)}{\partial y(t_k)} \tag{53}$$

$$\frac{\partial g_{2s}(t_i)}{\partial z(t_k)} = \frac{\partial g_{2s}(t_i)}{\partial x_s(t_i)}\frac{\partial x_s(t_i)}{\partial z(t_k)} + \frac{\partial g_{2s}(t_i)}{\partial y_s(t_i)}\frac{\partial y_s(t_i)}{\partial z(t_k)} + \frac{\partial g_{2s}(t_i)}{\partial z_s(t_i)}\frac{\partial z_s(t_i)}{\partial z(t_k)} \tag{54}$$

$$\frac{\partial g_{2s}(t_i)}{\partial \psi_k} = \frac{\partial g_{2s}(t_i)}{\partial x_s(t_i)}\frac{\partial x_s(t_i)}{\partial \psi_k} + \frac{\partial g_{2s}(t_i)}{\partial y_s(t_i)}\frac{\partial y_s(t_i)}{\partial \psi_k} + \frac{\partial g_{2s}(t_i)}{\partial z_s(t_i)}\frac{\partial z_s(t_i)}{\partial \psi_k} \tag{55}$$

$$\frac{\partial g_{2s}(t_i)}{\partial \rho_k} = \frac{\partial g_{2s}(t_i)}{\partial x_s(t_i)}\frac{\partial x_s(t_i)}{\partial \rho_k} + \frac{\partial g_{2s}(t_i)}{\partial y_s(t_i)}\frac{\partial y_s(t_i)}{\partial \rho_k} + \frac{\partial g_{2s}(t_i)}{\partial z_s(t_i)}\frac{\partial z_s(t_i)}{\partial \rho_k} \tag{56}$$

$$\frac{\partial g_{2s}(t_i)}{\partial \phi_k} = \frac{\partial g_{2s}(t_i)}{\partial x_s(t_i)}\frac{\partial x_s(t_i)}{\partial \phi_k} + \frac{\partial g_{2s}(t_i)}{\partial y_s(t_i)}\frac{\partial y_s(t_i)}{\partial \phi_k} + \frac{\partial g_{2s}(t_i)}{\partial z_s(t_i)}\frac{\partial z_s(t_i)}{\partial \phi_k} \tag{57}$$

Given that (2) can be written as

$$\begin{aligned}\mathbf{x}_s(t_i) &= \begin{bmatrix} x_s(t_i) \\ y_s(t_i) \\ z_s(t_i) \end{bmatrix} = T_s(\mathbf{x}(t_i) - \boldsymbol{\xi}_s) \\ &= \begin{bmatrix} T_{s_{11}} & T_{s_{12}} & T_{s_{13}} \\ T_{s_{21}} & T_{s_{22}} & T_{s_{23}} \\ T_{s_{31}} & T_{s_{32}} & T_{s_{33}} \end{bmatrix} \begin{bmatrix} x(t_i) - \xi_s \\ y(t_i) - \eta_s \\ z(t_i) - \zeta_s \end{bmatrix}\end{aligned} \tag{58}$$

therefore

$$x_s(t_i) = T_{s_{11}}(x(t_i) - \xi_s) + T_{s_{12}}(y(t_i) - \eta_s) + T_{s_{13}}(z(t_i) - \zeta_s) \tag{59}$$

$$y_s(t_i) = T_{s_{21}}(x(t_i) - \xi_s) + T_{s_{22}}(y(t_i) - \eta_s) + T_{s_{23}}(z(t_i) - \zeta_s) \tag{60}$$

$$z_s(t_i) = T_{s_{31}}(x(t_i) - \xi_s) + T_{s_{32}}(y(t_i) - \eta_s) + T_{s_{33}}(z(t_i) - \zeta_s) \tag{61}$$

and

$$\begin{aligned}&\frac{\partial x_s(t_i)}{\partial x(t_k)} = T_{s_{11}}, \quad \frac{\partial x_s(t_i)}{\partial y(t_k)} = T_{s_{12}}, \quad \frac{\partial x_s(t_i)}{\partial y(t_k)} = T_{s_{13}} \\ &\frac{\partial y_s(t_i)}{\partial x(t_k)} = T_{s_{21}}, \quad \frac{\partial y_s(t_i)}{\partial y(t_k)} = T_{s_{22}}, \quad \frac{\partial y_s(t_i)}{\partial y(t_k)} = T_{s_{23}} \\ &\frac{\partial z_s(t_i)}{\partial x(t_k)} = T_{s_{31}}, \quad \frac{\partial z_s(t_i)}{\partial y(t_k)} = T_{s_{32}}, \quad \frac{\partial z_s(t_i)}{\partial y(t_k)} = T_{s_{33}}\end{aligned} \tag{62}$$

$$\frac{\partial x_s(t_i)}{\partial \psi_k} = \frac{\partial T_{s_{11}}}{\partial \psi_k}(x(t_i) - \xi_s) + \frac{\partial T_{s_{12}}}{\partial \psi_k}(y(t_i) - \eta_s) + \frac{\partial T_{s_{13}}}{\partial \psi_k}(z(t_i) - \zeta_s) \tag{63}$$

$$\frac{\partial x_s(t_i)}{\partial \rho_k} = \frac{\partial T_{s_{11}}}{\partial \rho_k}(x(t_i) - \xi_s) + \frac{\partial T_{s_{12}}}{\partial \rho_k}(y(t_i) - \eta_s) + \frac{\partial T_{s_{13}}}{\partial \rho_k}(z(t_i) - \zeta_s) \tag{64}$$

$$\frac{\partial x_s(t_i)}{\partial \phi_k} = \frac{\partial T_{s_{11}}}{\partial \phi_k}(x(t_i) - \xi_s) + \frac{\partial T_{s_{12}}}{\partial \phi_k}(y(t_i) - \eta_s) + \frac{\partial T_{s_{13}}}{\partial \phi_k}(z(t_i) - \zeta_s) \tag{65}$$

$$\frac{\partial y_s(t_i)}{\partial \psi_k} = \frac{\partial T_{s_{21}}}{\partial \psi_k}(x(t_i) - \xi_s) + \frac{\partial T_{s_{22}}}{\partial \psi_k}(y(t_i) - \eta_s) + \frac{\partial T_{s_{23}}}{\partial \psi_k}(z(t_i) - \zeta_s) \tag{66}$$

$$\frac{\partial y_s(t_i)}{\partial \rho_k} = \frac{\partial T_{s_{21}}}{\partial \rho_k}(x(t_i) - \xi_s) + \frac{\partial T_{s_{22}}}{\partial \rho_k}(y(t_i) - \eta_s) + \frac{\partial T_{s_{23}}}{\partial \rho_k}(z(t_i) - \zeta_s) \tag{67}$$

$$\frac{\partial y_s(t_i)}{\partial \phi_k} = \frac{\partial T_{s_{11}}}{\partial \phi_k}(x(t_i) - \xi_s) + \frac{\partial T_{s_{22}}}{\partial \phi_k}(y(t_i) - \eta_s) + \frac{\partial T_{s_{23}}}{\partial \phi_k}(z(t_i) - \zeta_s) \tag{68}$$

$$\frac{\partial z_s(t_i)}{\partial \psi_k} = \frac{\partial T_{s_{31}}}{\partial \psi_k}(x(t_i) - \xi_s) + \frac{\partial T_{s_{32}}}{\partial \psi_k}(y(t_i) - \eta_s) + \frac{\partial T_{s_{33}}}{\partial \psi_k}(z(t_i) - \zeta_s) \tag{69}$$

$$\frac{\partial z_s(t_i)}{\partial \rho_k} = \frac{\partial T_{s_{31}}}{\partial \rho_k}(x(t_i) - \xi_s) + \frac{\partial T_{s_{32}}}{\partial \rho_k}(y(t_i) - \eta_s) + \frac{\partial T_{s_{33}}}{\partial \rho_k}(z(t_i) - \zeta_s) \tag{70}$$

$$\frac{\partial z_s(t_i)}{\partial \phi_k} = \frac{\partial T_{s_{31}}}{\partial \phi_k}(x(t_i) - \xi_s) + \frac{\partial T_{s_{32}}}{\partial \phi_k}(y(t_i) - \eta_s) + \frac{\partial T_{s_{33}}}{\partial \phi_k}(z(t_i) - \zeta_s) \tag{71}$$

$$\frac{\partial g_{1s}(t_i)}{\partial x_s(t_i)} = \frac{z_s(t_i)}{z_s(t_i)^2 + x_s(t_i)^2} \tag{72}$$

$$\frac{\partial g_{1s}(t_i)}{\partial y_s(t_i)} = 0 \tag{73}$$

$$\frac{\partial g_{1s}(t_i)}{\partial z_s(t_i)} = -\frac{x_s(t_i)}{x_s(t_i)^2 + z_s(t_i)^2} \tag{74}$$

$$\frac{\partial g_{2s}(t_i)}{\partial x_s(t_i)} = -\frac{x_s(t_i)y_s(t_i)}{\sqrt{(x_s(t_i)^2 + z_s(t_i)^2)}(x_s(t_i)^2 + y_s(t_i)^2 + z_s(t_i)^2)} \tag{75}$$

$$\frac{\partial g_{2s}(t_i)}{\partial y_s(t_i)} = \frac{\sqrt{x_s(t_i)^2 + z_s(t_i)^2}}{x_s(t_i)^2 + y_s(t_i)^2 + z_s(t_i)^2} \tag{76}$$

$$\frac{\partial g_{2s}(t_i)}{\partial z_s(t_i)} = -\frac{z_s(t_i)y_s(t_i)}{(x_s(t_i)^2 + y_s(t_i)^2 + z_s(t_i)^2)(\sqrt{x_s(t_i)^2 + z_s(t_i)^2})} \tag{77}$$

$$\frac{\partial T_{s_{11}}}{\partial \psi_k} = -\sin\psi_k \cos\rho_k \tag{78}$$

$$\frac{\partial T_{s_{12}}}{\partial \psi_k} = -\sin\psi_k \sin\rho_k \sin\phi_k - \cos\psi_k \cos\phi_k \tag{79}$$

$$\frac{\partial T_{s_{13}}}{\partial \psi_k} = -\sin\psi_k \sin\rho_k \cos\phi_k + \cos\psi_k \sin\phi_k \tag{80}$$

$$\frac{\partial T_{s_{21}}}{\partial \psi_k} = \cos\psi_k \cos\rho_k \tag{81}$$

$$\frac{\partial T_{s_{22}}}{\partial \psi_k} = \cos\psi_k \sin\rho_k \sin\phi_k - \sin\psi_k \cos\phi_k \tag{82}$$

$$\frac{\partial T_{s_{23}}}{\partial \psi_k} = \cos\psi_k \sin\rho_k \cos\phi_k + \sin\psi_k \sin\phi_k \tag{83}$$

$$\frac{\partial T_{s_{31}}}{\partial \psi_k} = 0 \tag{84}$$

$$\frac{\partial T_{s_{32}}}{\partial \psi_k} = 0 \tag{85}$$

$$\frac{\partial T_{s_{33}}}{\partial \psi_k} = 0 \tag{86}$$

$$\frac{\partial T_{s_{11}}}{\partial \rho_k} = -\cos\psi_k \sin\rho_k \tag{87}$$

$$\frac{\partial T_{s_{12}}}{\partial \rho_k} = \cos\psi_k \cos\rho_k \sin\phi_k \tag{88}$$

$$\frac{\partial T_{s_{13}}}{\partial \rho_k} = \cos\psi_k \cos\rho_k \cos\phi_k \tag{89}$$

$$\frac{\partial T_{s_{21}}}{\partial \rho_k} = -\sin\psi_k \sin\phi_k \tag{90}$$

$$\frac{\partial T_{s_{22}}}{\partial \rho_k} = \sin\psi_k \cos\rho_k \sin\phi_k \tag{91}$$

$$\frac{\partial T_{s_{23}}}{\partial \rho_k} = \sin\psi_k \cos\rho_k \cos\phi_k \tag{92}$$

$$\frac{\partial T_{s_{31}}}{\partial \rho_k} = -\cos\phi_k \tag{93}$$

$$\frac{\partial T_{s_{32}}}{\partial \rho_k} = -\sin\rho_k \sin\phi_k \tag{94}$$

$$\frac{\partial T_{s_{33}}}{\partial \rho_k} = -\sin\rho_k \cos\phi_k \tag{95}$$

$$\frac{\partial T_{s_{11}}}{\partial \phi_k} = 0 \tag{96}$$

$$\frac{\partial T_{s_{12}}}{\partial \phi_k} = \cos\psi_k \sin\rho_k \cos\phi_k + \sin\psi_k \sin\phi_k \tag{97}$$

$$\frac{\partial T_{s_{13}}}{\partial \phi_k} = -\cos\psi_k \sin\rho_k \sin\phi_k + \sin\psi_k \cos\phi_k \tag{98}$$

$$\frac{\partial T_{s_{21}}}{\partial \phi_k} = 0 \tag{99}$$

$$\frac{\partial T_{s_{22}}}{\partial \phi_k} = \sin\psi_k \sin\rho_k \cos\phi_k - \cos\psi_k \sin\phi_k \tag{100}$$

$$\frac{\partial T_{s_{23}}}{\partial \phi_k} = -\sin\psi_k \sin\rho_k \sin\phi_k - \cos\psi_k \cos\phi_k \tag{101}$$

$$\frac{\partial T_{s_{31}}}{\partial \phi_k} = 0 \tag{102}$$

$$\frac{\partial T_{s_{32}}}{\partial \phi_k} = \cos\psi_k \cos\phi_k \tag{103}$$

$$\frac{\partial T_{s_{33}}}{\partial \phi_k} = -\cos\rho_k \sin\phi_k \tag{104}$$

REFERENCES

[1] Y. Bar-Shalom, X.-R. Li, and T. Kirubarajan
Estimation with Applications to Tracking and Navigation: Theory, Algorithms and Software.
Wiley, 2001.

[2] D. Belfadel, R. W. Osborne, and Y. Bar-Shalom
"A Minimalist Approach to Bias Estimation for Passive Sensor Measurements with Targets of Opportunity,"
in *Proc. SPIE Conf. Signal and Data Processing of Small Targets*, #8857-13, San Diego, California, Aug. 2013.

[3] D. Belfadel, R. W. Osborne, and Y. Bar-Shalom
"Bias Estimation for Optical Sensor Measurements with Targets of Opportunity,"
in *Proc. FUSION Conf.*, Istanbul, Turkey, July 2013.

[4] D. Belfadel, R. W. Osborne, and Y. Bar-Shalom
"Bias Estimation and Observability for Optical Sensor Measurements with Targets of Opportunity,"
Journal of Advances in Information Fusion, vol. 9, no. 2, pp. 59–74, Dec. 2014.

[5] T. M. Clemons and K.-C. Chang
"Sensor Calibration using In-Situ Celestial Observations to Estimate Bias in Space-Based Missile Tracking,"
IEEE Trans. on Aerospace and Electronic Systems, vol. 48, no. 2, pp. 1403–1427, April 2012.

[6] B. D. Kragel, S. Danford, S. M. Herman, and A. B. Poore
"Bias Estimation Using Targets of Opportunity,"
Proc. SPIE Conf. on Signal and Data Processing of Small Targets, #6699, Aug. 2007.

[7] B. D. Kragel, S. Danford, S. M. Herman, and A. B. Poore "Joint MAP Bias Estimation and Data Association: Algorithms," *Proc. SPIE Conf. on Signal and Data Processing of Small Targets*, #6699-1E, Aug. 2007.

[8] B. D. Kragel, S. Danford, and A. B. Poore "Concurrent MAP Data Association and Absolute Bias Estimation with an Arbitrary Number of Sensors," *Proc. SPIE Conf. on Signal and Data Processing of Small Targets*, #6969-50, May 2008.

[9] R. W. Osborne, III, and Y. Bar-Shalom "Statistical Efficiency of Composite Position Measurements from Passive Sensors," in *Proc. SPIE Conf. on Signal Proc., Sensor Fusion, and Target Recognition*, #8050-07, Orlando, FL, April 2011.

[10] R. W. Osborne, III, and Y. Bar-Shalom "Statistical Efficiency of Composite Position Measurements from Passive Sensors," *IEEE Tans. on Aerospace and Electronic Systems*, vol. 49, no. 4, Oct. 2013.

Djedjiga Belfadel is a Ph.D. candidate in the Electrical Engineering department at the University of Connecticut, Storrs, CT. Her research interests include target tracking, data association, sensor fusion, sensor biases, machine vision, and other aspects of estimation. She obtained her B.S., degrees from the University of Mouloud Mammeri in 2003, and her M.S., degrees from the University of New Haven in 2008, both in electrical engineering. Before joining the Estimation and Signal Processing (ESP) Laboratory, she worked, as an Electrical Engineer, from 2009 to 2011, at Evax Systems Inc. in Branford, Connecticut.

Richard W. Osborne, III obtained his B.S., M.S., and Ph.D. degrees in electrical engineering from the University of Connecticut in 2004, 2007, and 2012, respectively. From 2012–2014 he was an Assistant Research Professor in the Electrical Engineering department at the University of Connecticut, Storrs, CT. Currently, he is a Senior Research Engineer at BAE Systems, Inc. in Burlington, MA, working in the Performance, Exploitation and Dissemination (PED) Technology and Integration group. His academic interests include target tracking, information fusion, automated systems, and all aspects of estimation.

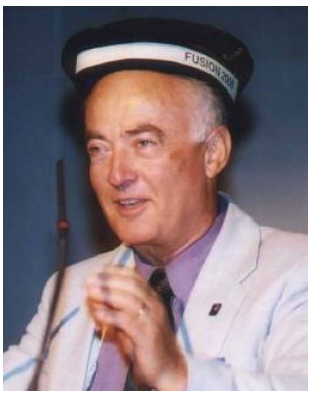

Yaakov Bar-Shalom was born on May 11, 1941. He received the B.S. and M.S. degrees from the Technion, Israel Institute of Technology, in 1963 and 1967 and the Ph.D. degree from Princeton University in 1970, all in electrical engineering. From 1970 to 1976 he was with Systems Control, Inc., Palo Alto, California. Currently he is Board of Trustees Distinguished Professor in the Dept. of Electrical and Computer Engineering and Marianne E. Klewin Professor in Engineering at the University of Connecticut. He is also Director of the ESP (Estimation and Signal Processing) Lab. His current research interests are in estimation theory, target tracking and data fusion. He has published over 500 papers and book chapters in these areas and in stochastic adaptive control. He coauthored the monograph Tracking and Data Association (Academic Press, 1988), the graduate texts Estimation and Tracking: Principles, Techniques and Software (Artech House, 1993), Estimation with Applications to Tracking and Navigation: Algorithms and Software for Information Extraction (Wiley, 2001), the advanced graduate texts Multitarget-Multisensor Tracking: Principles and Techniques (YBS Publishing, 1995), Tracking and Data Fusion (YBS Publishing, 2011), and edited the books Multitarget-Multisensor Tracking: Applications and Advances (Artech House, Vol. I, 1990; Vol. II, 1992; Vol. III, 2000). He has been elected Fellow of IEEE for "contributions to the theory of stochastic systems and of multi-target tracking." He has been consulting to numerous companies and government agencies, and originated the series of Multitarget-Multisensor Tracking short courses offered via UCLA Extension, at Government Laboratories, private companies and overseas. During 1976 and 1977 he served as Associate Editor of the IEEE Transactions on Automatic Control and from 1978 to 1981 as Associate Editor of Automatica. He was Program Chairman of the 1982 American Control Conference, General Chairman of the 1985 ACC, and Co-Chairman of the 1989 IEEE International Conference on Control and Applications. During 1983–87 he served as Chairman of the Conference Activities Board of the IEEE Control Systems Society and during 1987–89 was a member of the Board of Governors of the IEEE CSS. He was a member of the Board of Directors of the International Society of Information Fusion (1999–2004) and served as General Chairman of FUSION 2000, President of ISIF in 2000 and 2002 and Vice President for Publications in 2004–13. In 1987 he received the IEEE CSS Distinguished Member Award. Since 1995 he is a Distinguished Lecturer of the IEEE AESS and has given numerous keynote addresses at major national and international conferences. He is co-recipient of the M. Barry Carlton Award for the best paper in the IEEE Transactions on Aerospace and Electronic Systems in 1995 and 2000 and recipient of the 1998 University of Connecticut AAUP Excellence Award for Research. In 2002 he received the J. Mignona Data Fusion Award from the DoD JDL Data Fusion Group. He is a member of the Connecticut Academy of Science and Engineering. In 2008 he was awarded the IEEE Dennis J. Picard Medal for Radar Technologies and Applications, and in 2012 the Connecticut Medal of Technology. He has been listed by academic.research.microsoft (top authors in engineering) as #1 among the researchers in Aerospace Engineering based on the citations of his work.